Colloid Polym Sci (2002) 280: 1067–1074
DOI 10.1007/s00396-002-0739-3

ORIGINAL CONTRIBUTION

Ruggero Micheletto
Jun Matsui
Nobuki Yoshimatsu
Munetaka Oyama
Satoshi Okazaki

Study of the fluorescence of perylene cation radical salts with a near field optical setup

Received: 11 March 2002
Revised: 30 April 2002
Accepted: 7 May 2002
Published online: 19 July 2002

R. Micheletto (✉) · J. Matsui
N. Yoshimatsu · M. Oyama · S. Okazaki
Kyoto University,
Graduate School of Engineering,
Department of Material Chemistry,
Sakyo-ku, Yoshida, 606–8501 Kyoto,
Japan
E-mail: Ruggero@mc.kyoto-u.ac.jp
Tel.: +81.75.753.5883
Fax: +81.75.753.4718

Abstract A perylene-acetonitrile solution with TBAP (tetra-n-butylammonium perchlorate) electrocrystallizes on the electrode surface, under opportune conditions. It forms particular needle-like microcrystals that have been studied recently for their peculiar electrical and optical properties and for the fundamental processes involved in the electron transfer responsible for the electrocrystallization. These intriguing structures present various fractal-like morphological organizations and diverse crystal shapes on the same deposition process. Up to now these formations have been studied optically by conventional standard microscopy. We introduce here a novel methodology to collect information on the actual orientation and crystal structure by a near field optical setup with originally fabricated probes. We performed, for the first time on these samples, near field fluorescence imaging showing evidence that the perylene aggregations actually have a distinct optical orientation.

Keywords SNOM · Perylene · Crystals · Electrocrystallization · Orientation

Introduction

The trend towards the fabrication of new miniaturized devices with desirable electronic characteristics has led to extensive investigations of molecular solids, that is, solids designed on the basis of molecular principles. These materials contain discrete components that have been condensed into an organized framework as a result of intermolecular interactions, crystal forces, or van der Waals forces. The interest in these materials is focused on the investigation of structure-function relationships that would facilitate the modification of their physical and electronic properties through rational approaches, possibly helping the design of molecular-scale electronic devices [1, 2]. These materials generally present unique ordered crystalline lattices characterized by a quasi-one-dimensional structure [3]. Geometrical properties associated with a uniform composition of discrete molecules give them particular optoelectronic properties, such as non-linear optical phenomena arising from unique lattice structures and intermolecular interactions [4].

We studied here a specific molecular solid, the perylene cation radical salts obtained through electrocrystallization. This solid is formed during the electrochemical oxidation on the cathode (described later) resulting in a dimer cation radical crystal growth progression at the electrode. The intriguing structures formed have been investigated in a number of studies [5, 6, 7]. However, the fundamental process of growth has not been explained completely. In the effort to elucidate these mechanisms we considered that with conventional high-resolution systems such as SEM (or STM, AFM), it is not possible to directly see the inner molecular organization of the different crystals. However, an optical technique could give many interesting insights on the molecular arrangement, simply probing the local optical properties of the aggregation under study. We introduce here a novel way to investigate these crystal formations

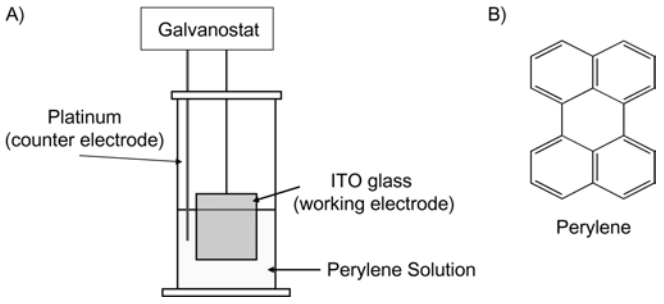

Fig. 1 **A** Scheme showing the process of electrocrystallization realized in the cell.. A galvanostat applies a constant current in the cell in order to induce the deposition of perylene cation radical salts on the ITO treated glass electrode (constant current of 0.5 mA). The solution indicated is 0.1 M TBAP, 1 mM perilene in acetonitrile, see text for details. **B** The molecular structure of perylene

using a SNOM (scanning near field optical microscope) to probe the optical and fluorescence properties of these materials in the optical near field range. The system we developed allows us not only to detect the profile of the crystals, but also to sense other optical information in order to contribute to the understanding of their inner composition. In particular, we performed fluorescence spectroscopy and fluorescence near field imaging, deducing for the first time information on the crystal orientation within the aggregation structures.

Experimental

We produced the perylene cation radical salts under investigation following a previously developed electrochemical technique [6]. In Fig. 1 we show a schematic diagram of the setup. In an undivided cell (a 500 ml beaker) we inserted two electrodes, one electrode was an ITO (indium tin oxide) treated glass (Asahi Optics, Japan), connected to the cathode of a battery, acting as working electrode. As counter electrode on the other side, a platinum rod was connected to the anode. The solution in which the electro deposition took place was 1 mM perylene, 0.1 M TBAP (tetra-n-butylammonium perchlorate) in acetonitrile. The solution was electrolyzed by a constant current of 0.5 mA. Perylene (Pe) is oxidized on the working electrode (ITO glass) in a reaction that generated an oxidative deposition of perylene dimer cation radical ($Pe^{\cdot+}$). The electrocrystallization process can be described as follows:

$$Pe \rightleftharpoons Pe^{\cdot+} + e^{-}$$

$$Pe^{\cdot+}ClO_4^{-} \rightleftharpoons PeClO_4\,(\text{crystalline})$$

In the process, the ClO_4^- salt of perylene cation radical crystallized on the electrode surface at a relatively slow rate. We controlled the crystal growth by the electrolysis time, 0.1–10 s, obtaining needle-like structures of different lengths. The overall length of the needle-like micro crystals was found to increase with the oxidation time.

We observed the arrangements obtained at different scales with a conventional optical microscope (Fig. 2) and with a scanning electron microscope (SEM), Fig. 3. We noticed that the structure of the crystals was different at different scales: needle-like quasi

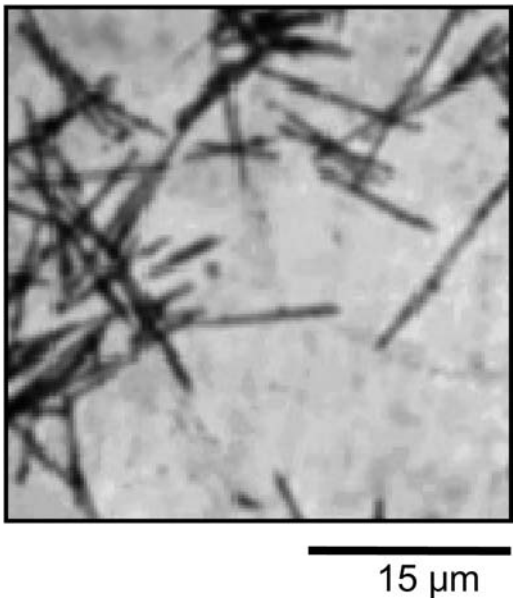

Fig. 2 An image of the crystallizations found on the ITO electrode surface after oxidation had occurred for 10 s. The image has been taken by a conventional optical microscope

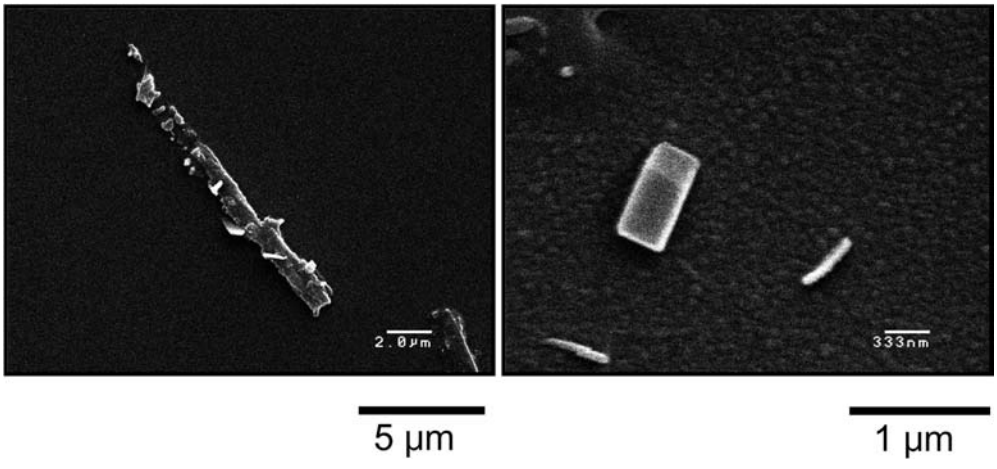

Fig. 3A–B Two SEM pictures of the crystals. **A** An isolated needle-like microcrystal. **B** One nano-sized crystals that are formed on the electrode. These smaller crystals have different shapes, elongated structures (needle in the *center right* or *bottom left*) or bulky regular objects like the one in the *center left*

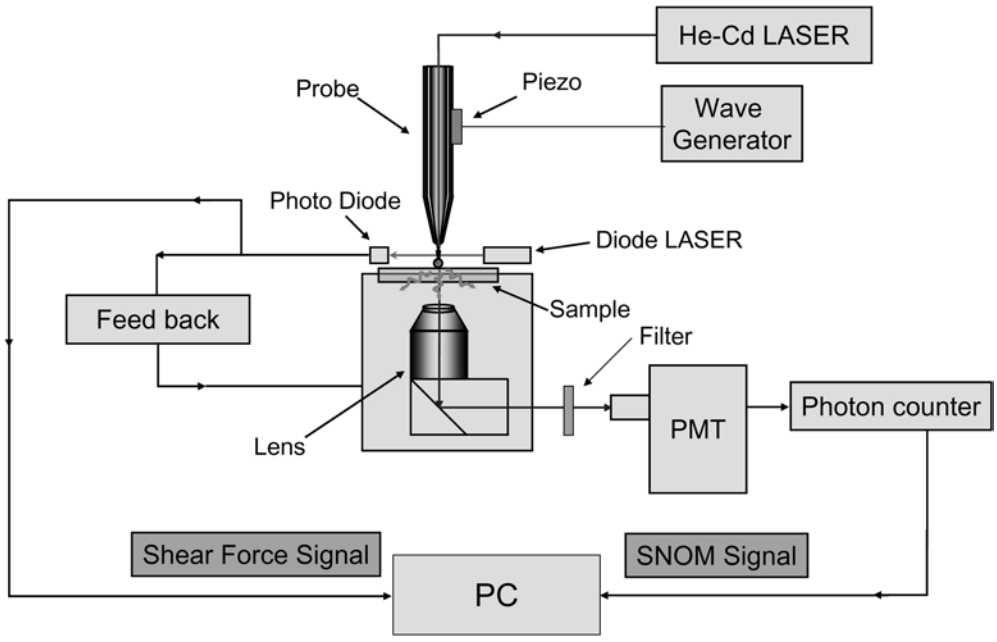

Fig. 4 Block diagram of the SNOM apparatus used in the experiments

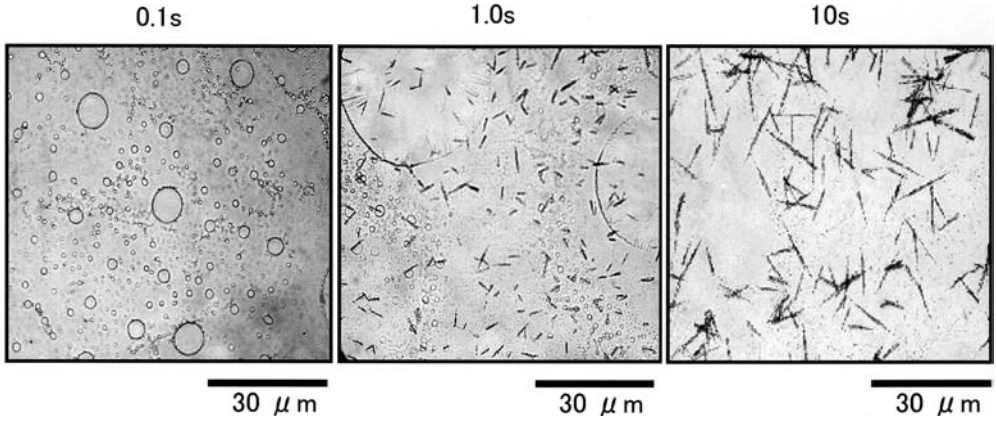

Fig. 5 Three different optical microscope pictures of the crystallization on the ITO glass electrode. After 10 s of electro-oxidation we see the rod like structures clearly formed. For shorter times (1.0 s and 0.1 s) we see smaller crystals.In the case of 0.1 s, there are practically no visible formations. The *circular structures* in the pictures, corresponding to 0.1 s and 1.0 s, are artifacts, presumably due to uneven evaporation of the solvent

one-dimensional in the micron scale, regular cubic or parallelepiped-like structures at smaller scales down to a few hundredths of a nanometer. As mentioned above, SEM or other non-optical techniques do not give direct information about the inner molecular orientation of the sample. So we arranged a near field experiment as described in the sketch in Fig. 4. The setup is based on a commercial SNOM apparatus [8], fitted with a glass near field probe. We originally fabricated our probes from commercial communication optical fibers of 125 microns diameter [9] with an aperture of about 100 nm and optical resolution in the same range. The optical alignment is as conventional illumination mode [10]. Additionally, the probe can be moved to a position of interest on the sample, and specific measurements, like spectroscopy or fluorescence, can be performed at that place.

Results and discussion

First of all, we prepared a series of electrocrystallizations and modified the duration of the electrolysis process in order to confirm the increased length of the needle-like structures with time, in the same fashion as described above. In Fig. 5 we show some optical images of the formation obtained. It is evident how the growing process proceeds with time. After several trials we fixed the electrolysis time to 10 s because with this value we had abundant crystal aggregations, large enough to be visualized easily by a conventional optical microscope, yet the sample was not too packed with crystals, so the actual shape of a single formation was easily distinguishable.

The structure of the crystals, as visible by optical microscope, presents a rod-like shape that looked as though it was covered with other smaller formations that appear as dark dots on the rod itself. To elucidate the nature of these, we decide then to examine the crystal at higher resolution by a SEM. In Fig. 6 we show two pictures of these aggregations shown by electron microscopy at different magnification. It is noticeable how the grow process of the main needle-like structures is accompanied by a number of substructures that join the

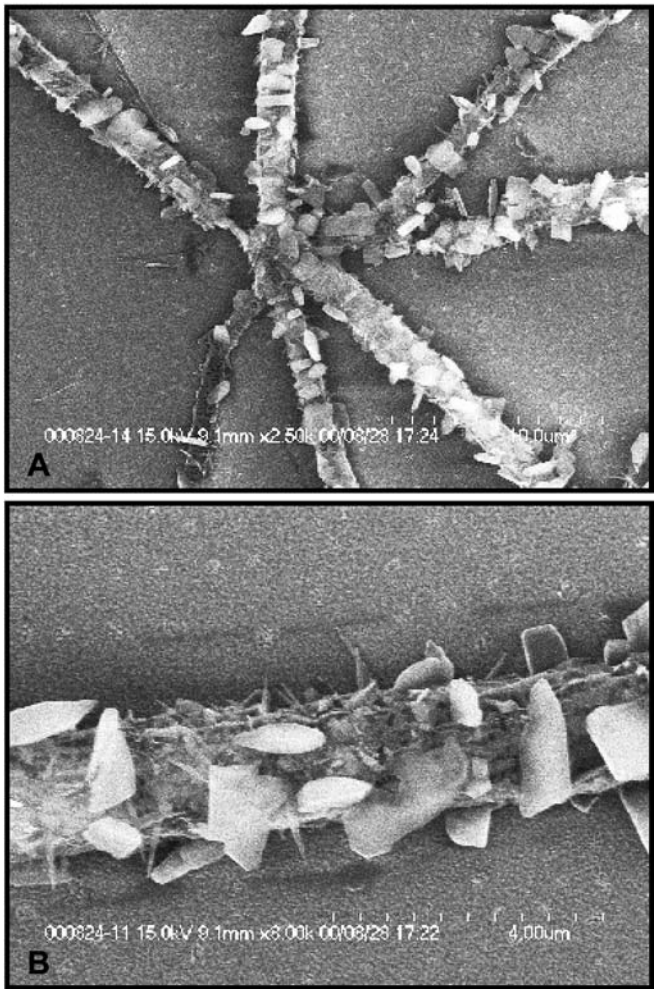

Fig. 6A–B Two SEM images at different scales of the perylene formation on the electrode. The image scales are **A** 20×15 μm and **B** 8×6 μm. The crystalline substructures discussed in the text are evident on the surface of the main needle-like formations

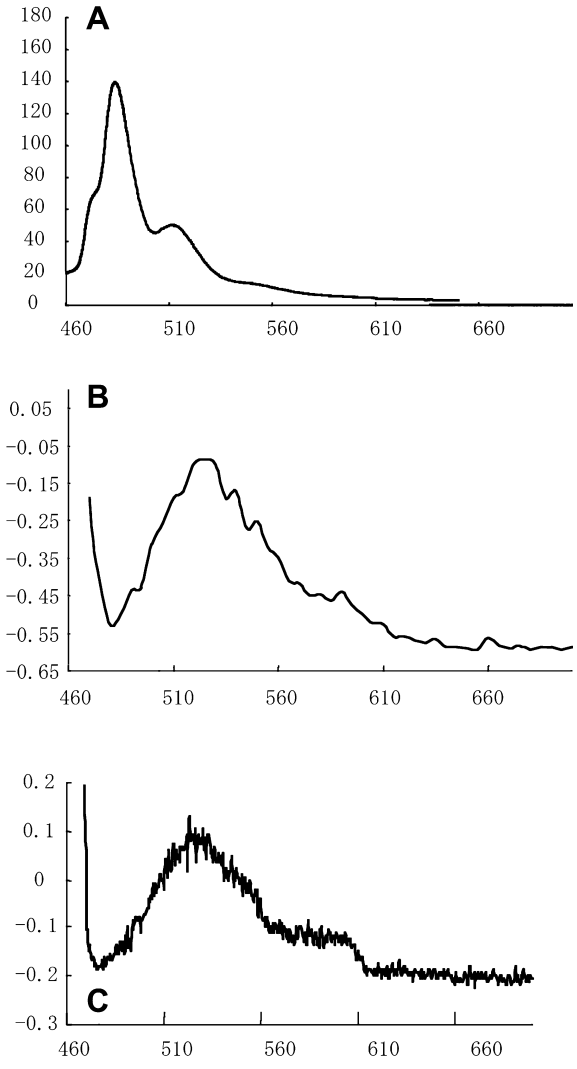

Fig. 7 **A** Fluorescence spectrum of perylene solution described in text. **B** The spectrum of the sample once crystallized on the ITO glass electrode. **C** Spectrum taken on the same sample as in **B** in near field condition. The emergence of a minor peak at 600 nm is noticeable. See text for discussion. The excitation light is 442 nm, from a 400 mW He-Cd laser. The transmitted light was collected underneath, filtering out the excitation light with a 480 nm color filter. The optical aperture of the original probes used to excite fluorescencefor **B** and **C** is of about 100 nm

aggregation forming a fractal-like object. This is a remarkable feature of the crystals that indicates the complexity of the growth phenomena in itself.

We measured the fluorescence properties of the sample in solution, then we assembled a complete fluorescence SNOM experiment in order to detect the fluorescence of the deposited crystals. See Fig. 7 for the spectrum of the sample in solution, and of the sample once deposited, analyzed in far and near field condition. The spectrum in solution (inset A) shows a peak at about 490 nm, which does not appear in the other two graphs (B and C). This is due to the major presence of the solvent acetonitrile; a secondary peak associated with the perylene molecule is visible at about 510 nm. The profile (inset B) is instead taken in far field on the dried crystallized sample. The peak related to the solvent is absent because it has been washed away and the measurement is performed in air. The secondary peak at about 510 nm is still visible, shifted slightly to higher wavelengths. We did not investigate the mechanism of this slight shift on lower energies. However, we consider that now the perylene molecule is crystallized and bounded as an ionic solid salt ($PeClO_4$), so there is no surprise that we have dissimilar energy gaps, resulting in a shift in the fluorescence emission pattern. In Fig 7C, we present the same measurement in near field condition, with the emitting probe at a few tenths of a nanometer from the actual crystalline structure. The

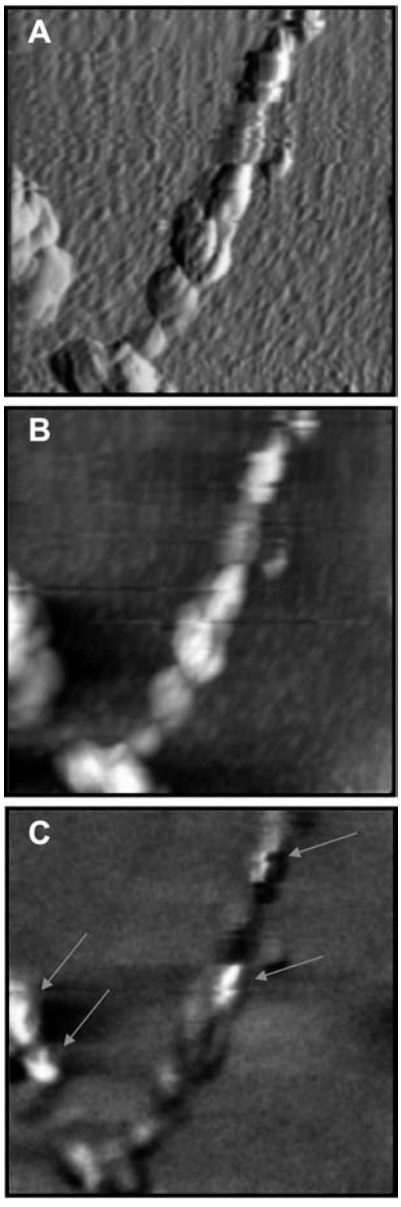

Fig. 8A–C Pictures of a crystal formation on ITO glass. The morphological information is represented in the two feedback signals in **A** and **B** (called respectively error or shear force, feedback or topo). The fluorescence optical signal is shown instead in **C**. Images are all 15×15 μm and composed of 256×256 pixels. Excitation wavelength is 442 nm. The *arrows* indicatethe regions of high intensity fluorescence emission discussed. These sites have no clear topological correspondence in **A** or **B**. Hence, the intense fluorescence is associated with the inner molecular orientation of the crystal. See discussion in the text

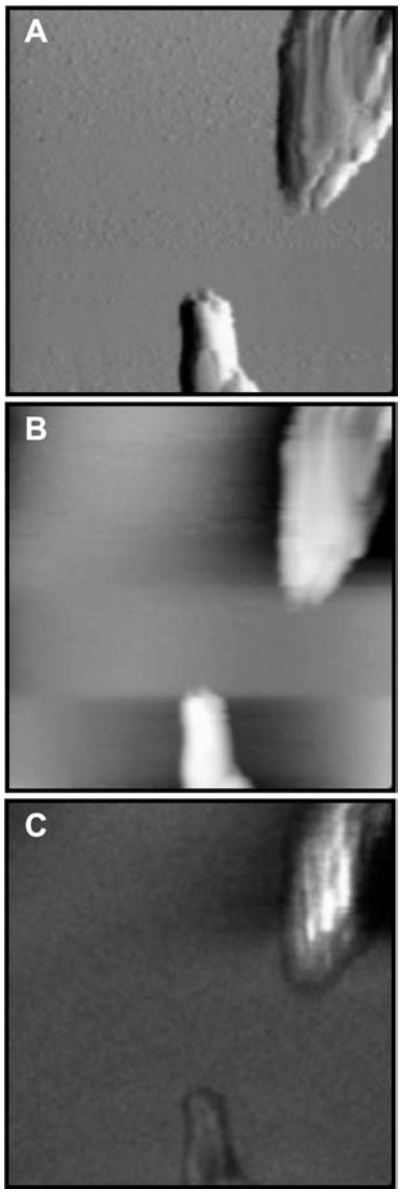

Fig. 9A–C Another example of similar crystal aggregations that behave optically quite differently. **A** Shear force map, **B** Topological map, **C** optical SNOM map. Images are all 15×15 μm and composed of 256×256 pixels. Excitation wavelength is 442 nm

profile is analogous, however, a minor peak at around 600 nm emerges. In near field configuration, the probe is extremely near to the sample and better coupling and improved sensitivity are realized. For this reason, peaks that are not detectable in conventional far field fluorescence are instead visible here. We do not yet know what is the nature of this peak; We leave this as an interesting experimental fact worth further investigation.

So far, we simply excited our crystals with an opportune light and measured the fluorescence emitted on a single location on the crystal. Hereafter, we will use our apparatus as a scanning microscope. The technique used is standard in near field optical microscopy. The tip is moved in a scanning fashion over the sample to

probe the separation constant by a conventional shear force controller [11]. A He-Cd laser (wavelength 442 nm, 400 mW power) illuminates the sample through the nano-sized aperture of our originally designed probe, inducing a fluorescence phenomenon confined in the region of the proximity of the tip. The total fluorescence light intensity is detected by a phototube placed under the sample, through a 480 nm color filter. In Fig. 8 we show the resulting scan over the crystal structures, which can be simply compared with the SEM images presented previously. It is noticeable how the fluorescence image profile shows some particular intense localized region of emissions indicated by arrows. These sites have no morphological correspondence in the actual crystal profile image (indicated in the picture insets A and B, representing the feedback error signal and the pure feedback signal). Comparing the SEM images with these ones, we can infer with a certain confidence that the tiny crystals growing on the body of the needle-like main structure may be responsible for these intense local emissions. As seen in Fig. 6B, these tiny crystals develop on the main ones in great number with various shapes and orientation. However, optically we observe only a few intense emission zones. This is interpretable as the molecular orientation of the structures that in certain fortunate cases couple strongly with the tip, and in most cases do not. In Fig. 9 we give another example of this phenomenon. The lower aggregation shown is darker than the upper in the optical scan. This is due to a different crystal orientation that is not favorable, and so there is a lower fluorescence emission in the direction of the detector. We show a qualitative sketch of this mechanism in Fig. 10.

We investigated this further, rotating the plane of vibration of the polarized light while observing a group of aggregations. As visible in Fig. 11A, while a bigger cluster maintains approximately the same emission intensity, two smaller ones show different fluorescence intensities depending on the angle of the excitation light (indicated by the arrow). The intensity transmitted seems to have a periodicity with the polarization angle; presumably this is simply due to optical polarization within the ordered molecular structures inside the crystal. As a purely qualitative interpretation, we consider the phenomenon to be a polarization by selective absorption problem [12]. So, we assume the presence in the crystal of a definite plane of transmission. The light is selectively transmitted through it and we can write the relation: $Q' = Q\ \mathrm{Cos}^2(a)$, the so-called Malus Law, where Q' is the intensity of the transmitted light (in our case the fluorescence signal), Q the intensity of the incident light and a the angle subtended by the two. If we indicate with E_i (the index i stands for the different polarization angles: 0°, 30°, 60°, and 90°) the various electric vectors representing the incident light, we can define α_i as the angle between them and the plane of transmission, then we can express the resulting intensity at the detector F as: $F = k\ E\ Cos^2(\alpha_i)$, where E is the module of E_i vectors (i.e. the intensity of the incident light) and k is a constant parameter representing the opacity of the material at that point. The observed intensity of the emission of the clusters in Fig. 11, appears to increase and decrease as the incident angle changes, within the 120° span of our measurement, so qualitatively in agreement with the discussion above.

We understand that the actual interaction process is rather complex. Particularly, we have to consider that

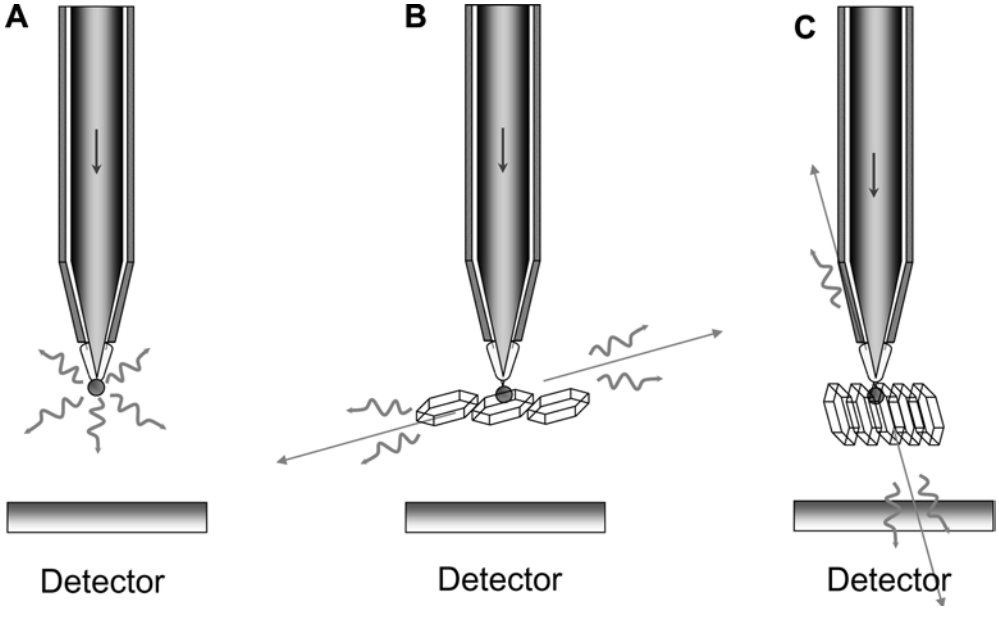

Fig. 10A–C A schematic representation of the mechanism discussed in the text. The molecular orientation of the aggregation enhances or reduces the coupling, resulting in an increased or reduced fluorescence at the detector. In **C** we represent the most favorable coupling condition: the crystal plane of transmission intersected the detector location. See discussion in the text

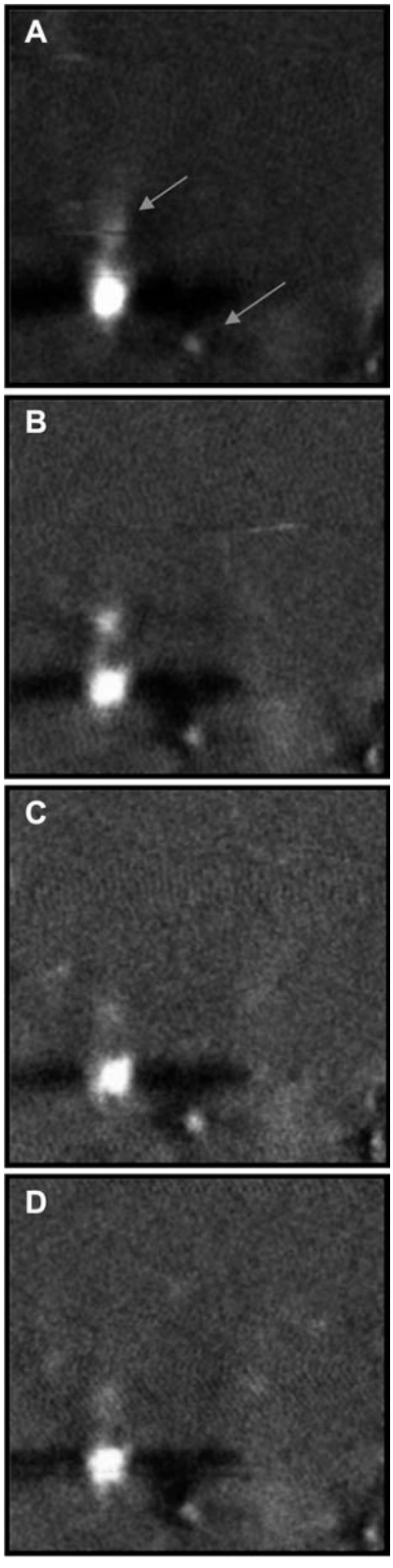

◀

Fig. 11A–D Four optical near field maps of the same perylene aggregations taken at different optical polarization. The clusters indicated with the *arrow* are polarization sensitive, and the detected fluorescence is variable depending on the polarization angle. The bigger cluster does not bear a particular orientation and its fluorescence appears approximately constant. Images are 7.5×7.5 μm and composed of 256×256 pixels. Angle of polarization of the excitation light is **A** 0°, **B** 30°, **C** 60°, and **D** 90°. The angle origin is arbitrary. Excitation wavelength is 442 nm

the linearly polarized incident light is inducing fluorescence and that this is the signal actually transmitted. Thus assuming that the Malus law is valid, we assume also that the fluorescence emission occurs in the same polarization plane of the incidence light. Also, the crystal orientation is presumably not perfect as there are surely dislocations and impurities of various natures that disturb the light propagation and induce intricate phenomena.

It would have been interesting to investigate further, extending the experiment to higher angles in order to observe a complete 180° cycle. Unfortunately this was not possible for mere experimental reasons: often we had evident deterioration of the tip and image quality in a single scan, and also slight drift in the position of the scan itself due to thermal reasons. The results shown in Fig. 11 were obtained after persevering in the same measurement, changing probes often, until four scans of reasonably good quality were acquired with the same tip.

Conclusions

We have introduced an original methodology to investigate the optical properties of perylene cation radicals deposited during the particular electro-oxidation process described. The method is based on the use of a near field optical microscope; it is general and applicable to other ionic crystals. We demonstrated that this approach is useful for optically revealing the actual structure of these intriguing materials. We studied the fluorescence emission of the sample in near field and far field conditions and we mapped the surface of the crystal in order to detect peculiar optical characteristics. Through analysis of the SNOM maps and by studying the behavior of the fluorescence versus the polarization of the incident light, we demonstrated (although qualitatively) that there are strong orientation optical phenomena in the crystal aggregations. In other words, the inner molecular orientation of certain structures strongly influences the optical coupling. We believe that the use of SNOM can be helpful to elucidate the fundamental properties of ionic solids and can contribute to the study of structure-function relationships of these fascinating materials that are potentially the basis for the fabrication of new miniaturized optical devices.

References

1. Lehen JM, Rees CW (eds) (1982) Molecular semiconductors. Springer, New York
2. Simon J, Andre JJ, Skoulios A (1986) J Nouv Chim 10:295
3. Miller JS (ed.) (1981–1983) Extended linear chain compounds vol 1–3
4. Eaton DF, Anderson AG, Tam W, Wang Y (1987) J Am Chem Soc 109:1886
5. Oyama M, Nitta Y, Okazaki S (2001) J Electroanal Chem 511:88
6. Oyama M, Mitani M, Washida, Masuda T, Okazaki S (1999) J Electroanal Chem. 473:166
7. Dittimer JJ et al., (2000) Solar energy materials and solar cells 61:53
8. Betzig E, Trautman JT (1992) Science 257:189
9. Micheletto R, Yoshimatsu N, Okazaki S, (2001) Optics Communications 188:11
10. Ohtsu M (1995) Optoelectronics Devices Technology 10/2:147
11. Betzig E, Trautman JK, Harris TD, Weiner JS, Kostelak RL (1991) Science 251:1468
12. Meyer-Arendt JR (1984) Introduction to classical and modern optics, Chap 3.4. Prentice-Hall